Int. J. Multiphase Flow Vol. 16, No. 3, pp. 375–390, 1990
Printed in Great Britain.

0301-9322/90 $3.00 + 0.00

MOTION OF LARGE GAS BUBBLES THROUGH LIQUIDS IN VERTICAL CONCENTRIC AND ECCENTRIC ANNULI

V. C. KELESSIDIS† and A. E. DUKLER‡
Department of Chemical Engineering, University of Houston, Houston, TX 77004, U.S.A.

(*Received* 1 *June* 1989; *in revised form* 6 *December* 1989)

Abstract—Taylor bubbles rising through liquids in vertical circular tubes and between parallel planes are axisymmetric and nearly spherical at the top. In a vertical annulus, however, the bubbles are radially asymmetric and never occupy the whole cross-sectional area. Analysis indicates that axisymmetric bubbles rise in an annulus at lower rates than those observed experimentally and hence are never observed in practice. In contrast, the asymmetric bubbles take an elliptic shape which results in higher rise velocities. A theoretical model for the rise velocity of an elliptic bubble has been developed and the comparison with experiment is satisfactory.

Key Words: Taylor bubbles, annulus, rise velocity

INTRODUCTION

It has long been known that gas–liquid flowing simultaneously in circular tubes can distribute in a variety of geometric patterns which depend on the flow rates, properties, tube diameter and inclination as well as flow direction relative to gravity (Dukler & Taitel 1986). Similar patterns exist when the conduit is an annulus. Experimental data and mechanistic models for predicting the conditions at which transitions take place from one flow pattern to another have recently been described for concentric and eccentric annuli (Kelessidis & Dukler 1989).

A flow pattern which exists over a wide range of flow rate space is that of slug flow. In a tube, slug flow is characterized by the pseudo periodic occurrence of large, bullet-shaped bubbles which have a round nose, a comparatively flat bottom, are positioned axisymmetrically and occupy most of the cross-sectional area of the tube. As the bubble rises, liquid flows around the bubble in a thin film moving along the wall. These are frequently designated as Taylor bubbles. Such Taylor bubbles also exist in a vertical annulus but the appearance is quite different, as shown in figure 1. The bubble having a round nose is wrapped around the inner tube occupying only part of the annular area. As the bubble rises liquid falls down in the annular space occupied by liquid as well as in thin films between the bubble and the tube walls.

This highly unsteady condition of slug flow can exist in a variety of situations of industrial importance where the flow configuration is that of an annulus. As examples, these conditions can be expected during drilling and logging operations in oil wells, in double-pipe heat exchangers where vaporization is taking place and in certain situations which can occur during emergency cooling of nuclear reactors. In order to design such systems or to interpret their performance, it is necessary to model slug flows. A central problem in such modeling is the need to predict the rise velocity of the Taylor bubbles (Fernandes *et al.* 1983). This paper is directed towards presenting experimental evidence and prediction of this rise velocity.

BACKGROUND

Study of the motion of Taylor bubbles through **stagnant liquid** in vertical tubes has generated a vast literature, starting with the pioneering contribution of Dumitrescu (1943) who considered

†Present address: Anadrill Schlumberger, Sugarland, TX 77478, U.S.A.
‡To whom all correspondence should be addressed.

the problem as one of potential flow around an axisymmetric cylinder having a rounded nose. Other significant contributions since that time using similar potential flow approaches include those of Davies & Taylor (1950), Collins (1965), Bendiksen (1985) and Nickens & Yanitell (1987) with many others in between. All these showed the existence of multiple solutions. However, by assuming the shape of the nose to be approximately spherical, all of these approaches produced a result similar to

$$U = K\sqrt{gD}, \qquad [1]$$

where the different investigators produced values of K ranging from 0.32 to 0.36, with U being the bubble rise velocity, D the tube diameter and g the acceleration of gravity. Recently, Mao & Dukler (1990) explored this problem using direct numerical simulation and were able to eliminate the ambiguity of the multiple solutions. For a Taylor bubble rising between closely-spaced parallel plates it is possible to take advantage of the simpler geometry and generate solutions for potential flow around the nose using mapping techniques. This approach was introduced by Birkhoff & Carter (1957) and followed by Garabedian (1957), Vanden-Broek (1984) and Couet *et al.* (1986). Again, the existence of multiple solutions to the mathematical problem was evident. All of these approaches ignored the viscous effects and these are expected to be especially important in thin receding films. Brown (1965) attempted to match the solution from potential flow to that for a receding viscous liquid film with only partial success. Of particular relevance to the work presented here is the contribution by Grace & Harrison (1967), who studied the effect of the frontal shape of the bubble on the rise velocity by considering bubbles enclosing a rod rising in a rectangular channel. Numerous experimental investigations in tubes and between parallel plates have also been carried out.

In a **flowing liquid** the rise velocity of a Taylor bubble clearly must depend on the velocity of the liquid upstream of the bubble as well as the relative motion due to buoyancy. Based on experimental data, Nicklin *et al.* (1962) suggested this relationship for situations where Re > 8000, where Re is the Reynolds number of the upstream flowing liquid:

$$U_N = 1.2U_M + 0.35\sqrt{gD}, \qquad [2]$$

where U_N is the propagation velocity of the Taylor bubble in flowing liquid and U_M is the cross-sectional average velocity of the upstream liquid. Since the coefficient of U_M is 1.2 for turbulent flow, this suggests that the effective upstream velocity is the centerline velocity of the liquid. Bendiksen (1984) carried out experiments to Re = 110,000, which confirmed this result of Nicklin *et al.* Collins *et al.* (1978) made the theoretical extension of the work of Dumitrescu (1943) for stagnant liquids to the case of flowing ones. While the theory suggests a somewhat different dependence than does [2], the practical result is about the same for low viscosity liquids.

Theoretical studies of Taylor bubbles rising through annuli are nonexistent, while experimental results are limited (Griffith 1964; Rader *et al.* 1975; Sadatomi *et al.* 1982) and lead to conflicting conclusions. Griffith and Sadatomi *et al.* both suggested using [1] with the effective diameter defined arbitrarily in a way that appeared to result in a fit with their data. Rader *et al.* correlated their data by replacing D in [1] with twice the measured radius of curvature of the nose.

EXPERIMENTAL EQUIPMENT

Measurements of the rise velocity, shape and the radial location of the bubble tip have been made in a vertical annulus consisting of an inside tube with o.d. = 0.0508 m and an outside tube with i.d. = 0.0762 m. The eccentricity of the annulus was adjustable and in these experiments was either 0 or 50%. The column length from the point of the air injection to the top of the column was 6.97 m. Details of the experimental equipment are given elsewhere (Kelessidis & Dukler 1989). Conductance probes were used for the rise velocity measurements. For two probes located a distance L apart vertically, the idealized output signal is depicted in figure 2. The times t_1, t_2 and t_3 can be measured and the rise velocity of the bubble, U, corrected for bubble expansion,

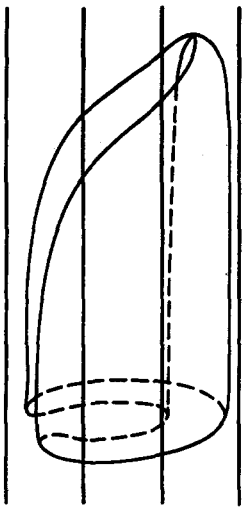

Figure 1. Schematic representation of a Taylor bubble rising in an annulus.

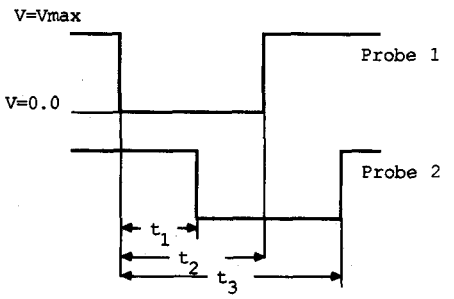

Figure 2. Conductance probe signal for the measurement of the rise velocity of a Taylor bubble.

is given by

$$U = \frac{\frac{L}{t_1}}{1 + \frac{\rho g t_2 L}{P t_1}}, \qquad [3]$$

where P is the static pressure at the position of the first probe and ρ is the liquid density. The length of the Taylor bubble, as detected by the two probes, may then be calculated by

$$l = Ut_2 = U(t_3 - t_1). \qquad [4]$$

Rise velocity measurements were made with stagnant liquid and flowing liquid using single Taylor bubbles as well as for continuously flowing gas and liquid (slug flow). For the first two cases, single Taylor bubbles were injected into the column using two solenoid valves operated by a dual set point electronic timer. Measurements of the rise velocity of different length Taylor bubbles were performed in order to determine the effect of the bubble length on the rise velocity.

The shape of single Taylor bubbles rising through stagnant and flowing liquid was determined using a set of 30 conductance probes placed 12° apart around the periphery. A schematic diagram of the probes and the electronics used is shown in figure 3. The voltage output gives the percentage of the periphery of the annulus occupied by the Taylor bubble. The rise velocity was measured simultaneously and the shape of the bubble in the azimuthal direction was obtained as a function of the axial distance from the bubble tip.

The radial location of the bubble tip was measured using four conductance probes placed across the gap of the concentric annulus (figure 4). The tip of the bubble will be located closest to the position of the probe that comes first into contact with the bubble. These resistance signals combined the measured rise velocity give a description of the bubble shape in the radial direction.

EXPERIMENTAL RESULTS

Velocity of the Taylor bubble

Measured velocities of single Taylor bubbles rising through stagnant liquid in the concentric and eccentric annulus (eccentricity 50%) are shown in figure 5. Each data point represents the average of measured velocities of at least 24 bubbles. The results indicate a weak dependence of the rise velocity on the bubble length for the concentric annulus and a somewhat stronger

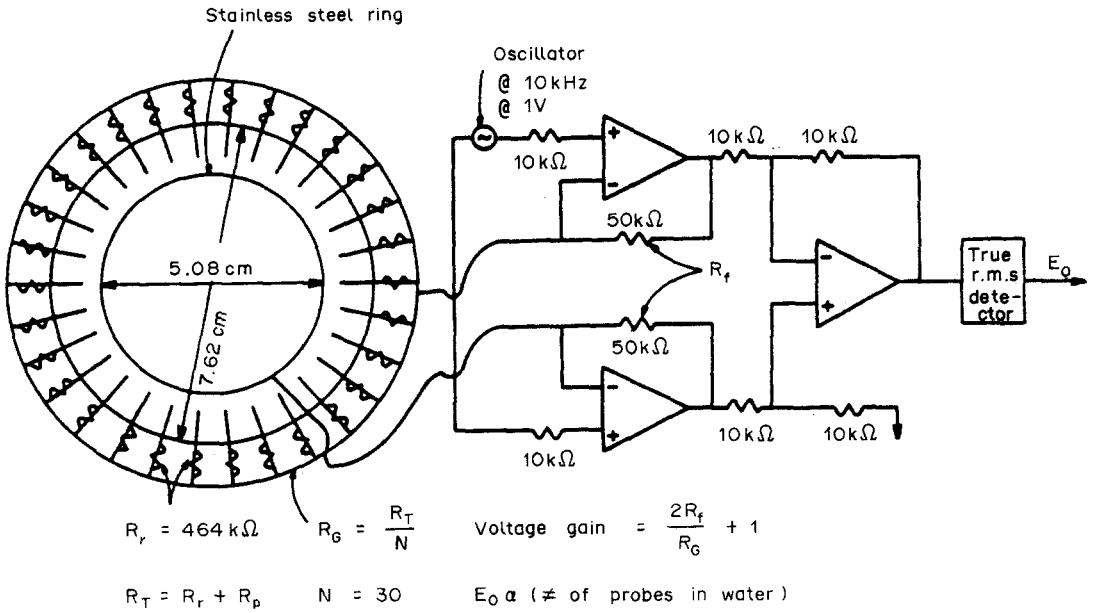

Figure 3. Schematic diagram of the probes and the circuit used for detection of the Taylor bubble shape.

dependence for the eccentric annulus. Linear regression for the two cases yields the following expressions:

$$U_C = 0.361 + 0.022l \text{ m/s}, \qquad R_c^2 = 0.946, \qquad [5]$$

and

$$U_E = 0.326 + 0.057l \text{ m/s}, \qquad R_c^2 = 0.987, \qquad [6]$$

where subscripts C and E represent the concentric and eccentric annulus configurations and R_c^2 is the correlation coefficient. Rader *et al.* (1975) found no significant effect of the bubble length on the rise velocity. It is speculated that slight changes in the bubble shape at the nose as the bubble gets longer and occupies more of the cross-sectional area, may be the cause of this effect.

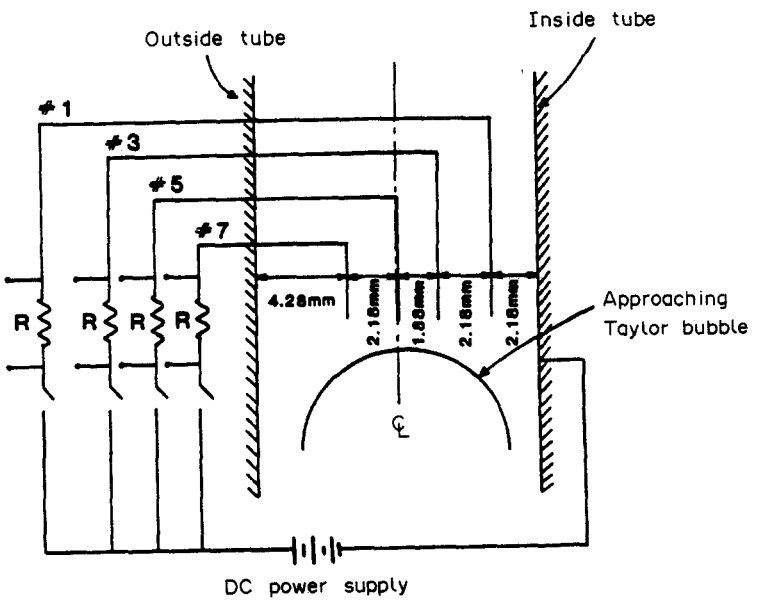

Figure 4. Schematic diagram of the probes for the detection of the position of the tip of the Taylor bubble in a concentric annulus.

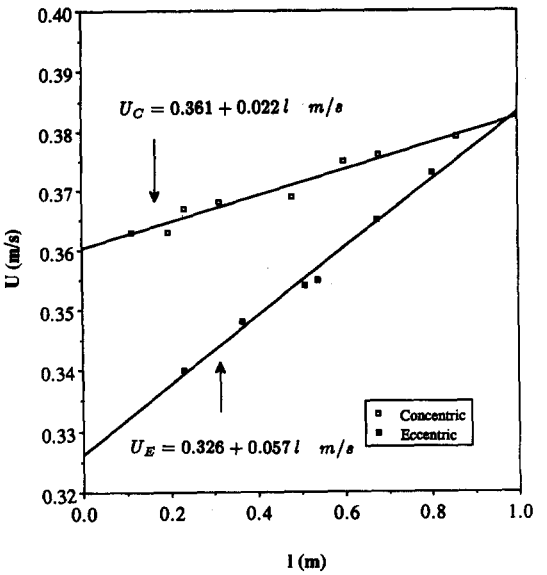

Figure 5. Rise velocity of different length Taylor bubbles in stagnant liquid in a concentric and an eccentric annulus.

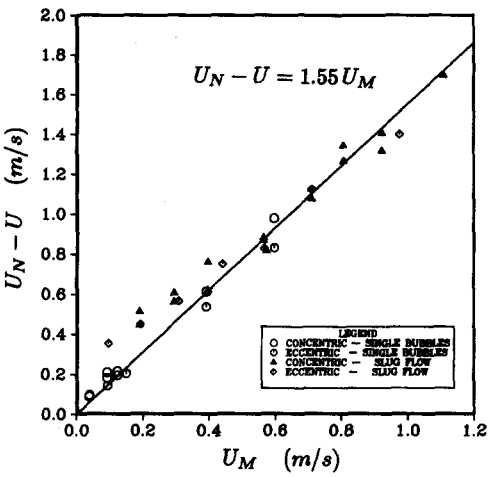

Figure 6. Average propagation velocity of a Taylor bubble in flowing liquid in an annulus.

The average values of the rise velocities in the concentric and eccentric annulus are 0.370 and 0.356 m/s, respectively.

The rise velocity of a Taylor bubble in a circular tube with the same diameter as the diameter of the outside tube of the annulus is approx. 0.30 m/s ([1] with $K = 0.35$). Hence, the rise velocities in concentric or eccentric annuli are considerably larger than the corresponding circular tube. Although data was taken with only one diameter ratio it is clear that the conclusion of Griffith (1964), that only the larger dimension is significant, is incorrect.

Data on the rise velocity of single Taylor bubbles injected into flowing liquid as well as data gathered during slug flow is shown in figure 6, where U is the predicted rise velocity in stagnant liquid, according to [5] and [6], and U_M is either the mixture velocity for slug flow or the average liquid velocity, $\bar{U}$, for single bubbles injected into flowing liquid. The data is reasonably well correlated by the equation

$$U_N - U = 1.55 U_M, \qquad R_c^2 = 0.96. \qquad [7]$$

It should be noted that $\mathrm{Re} = U_M D_h/\nu$, where D_h is the hydraulic diameter of the annulus and ν is the liquid kinematic viscosity, ranged from 1000 to 28,000 and [7] represents the data even at low Re, for which the flow is laminar. The coefficient of 1.55 in [7] is higher than the ratio of the maximum to the average liquid velocity for single-phase turbulent flow in an annulus. This is similar to the result found by Sadatomi *et al.* (1982). Previous investigators were not able to interpret the value of the coefficient for flow in an annulus in a manner similar to that for circular tubes (Griffith 1964; Sadatomi *et al.* 1982). One can speculate that the liquid velocity immediately ahead of the nose of the bubble increases from its maximum single-phase flow value due to the presence of the bubble. This velocity was measured in the concentric annulus using a hot film conical probe for three liquid flow rates. The results showed an increase in the liquid velocity ahead of the bubble tip but no conclusive evidence was found to relate this increase to the observed value of the coefficient.

The shape of the Taylor bubble

A plan view of the Taylor bubble in a concentric annulus is shown in figure 7. If $\phi = \theta/\pi$, ϕ is a monotonically increasing function of the axial distance, x, from the bubble tip. The conductance probes described above measure the quantity $1 - \phi$. As a result of the probe spacing, ϕ could be determined with $\pm 3.3\%$. The data was reduced by using the quantity S (figure 7) given by $S = \theta R_b$, where R_b is the radial position of the bubble tip. Since the bubble

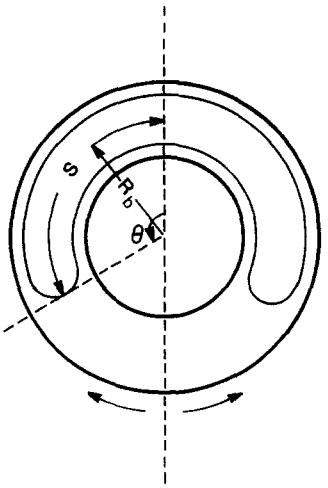

Figure 7. Plan view of a Taylor bubble rising in a concentric annulus.

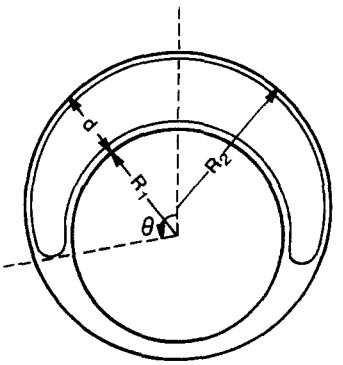

Figure 8. Plan view of a Taylor bubble rising in an eccentric annulus.

thickness is not known, R_b cannot be determined precisely. For a concentric annulus the bubble may be assumed radially symmetric so that

$$R_{bc} = \frac{R_1 + R_2}{2}, \qquad [8]$$

where R_1 and R_2 are the radii of the inner and outer tube, respectively. The plan view of the cross-sectional area of the Taylor bubble in the eccentric annulus is shown in figure 8. In this case

$$d = d_\theta = \sqrt{R_2^2 - e^2 \sin^2\theta} - R_1 + e\cos\theta \qquad [9]$$

and

$$R_{be} = R_1 + \frac{d_\theta}{2}. \qquad [10]$$

Experimental measurements of the bubble shape are shown in figures 9(a–f), where x is the vertical distance from the bubble tip. Different symbols indicate the shape of successive individual bubbles. Shapes are given here only for the vertical distance of 7 cm over which most of the change in shape was seen to occur. The solid lines in each plot represent an ellipse drawn through this same x distance. Attempts to fit a circle to the shape over this 7 cm were not possible, suggesting that a Taylor bubble rising in an annulus assumes the shape of an ellipse. For the eccentric annulus, the bubbles are more pointed at the nose and the major curvature occurs within a shorter distance from the bubble tip.

For each Taylor bubble, the maximum ϕ value, ϕ_l, was recorded and the measurements were averaged for each condition. The results for the stagnant and the flowing liquid cases are shown in figures 10 and 11, respectively. In the concentric annulus the bubble is symmetric in the azimuthal direction, hence, ϕ_l gives approximately the percentage of the area occupied by the bubble, neglecting the area occupied by the thin liquid films. This is not true, however, for the eccentric annulus, where the fraction of the cross-sectional area occupied by the bubble can be shown to be

$$\bar{\alpha}_e = \frac{\int_0^{\theta_l} [\sqrt{R_2^2 - e^2\sin^2\omega} + e\cos\omega]^2\, d\omega - \theta_l R_1^2}{\pi(R_2^2 - R_1^2)}, \qquad [11]$$

where $\theta_l = \phi_l \pi$. The data of figure 10 demonstrate that for stagnant liquid, the area occupied by the bubble is independent of the eccentricity and even for very short bubbles, the area occupied is over 70%. Even very long bubbles fail to completely enclose the inner tube. Bubbles approx.

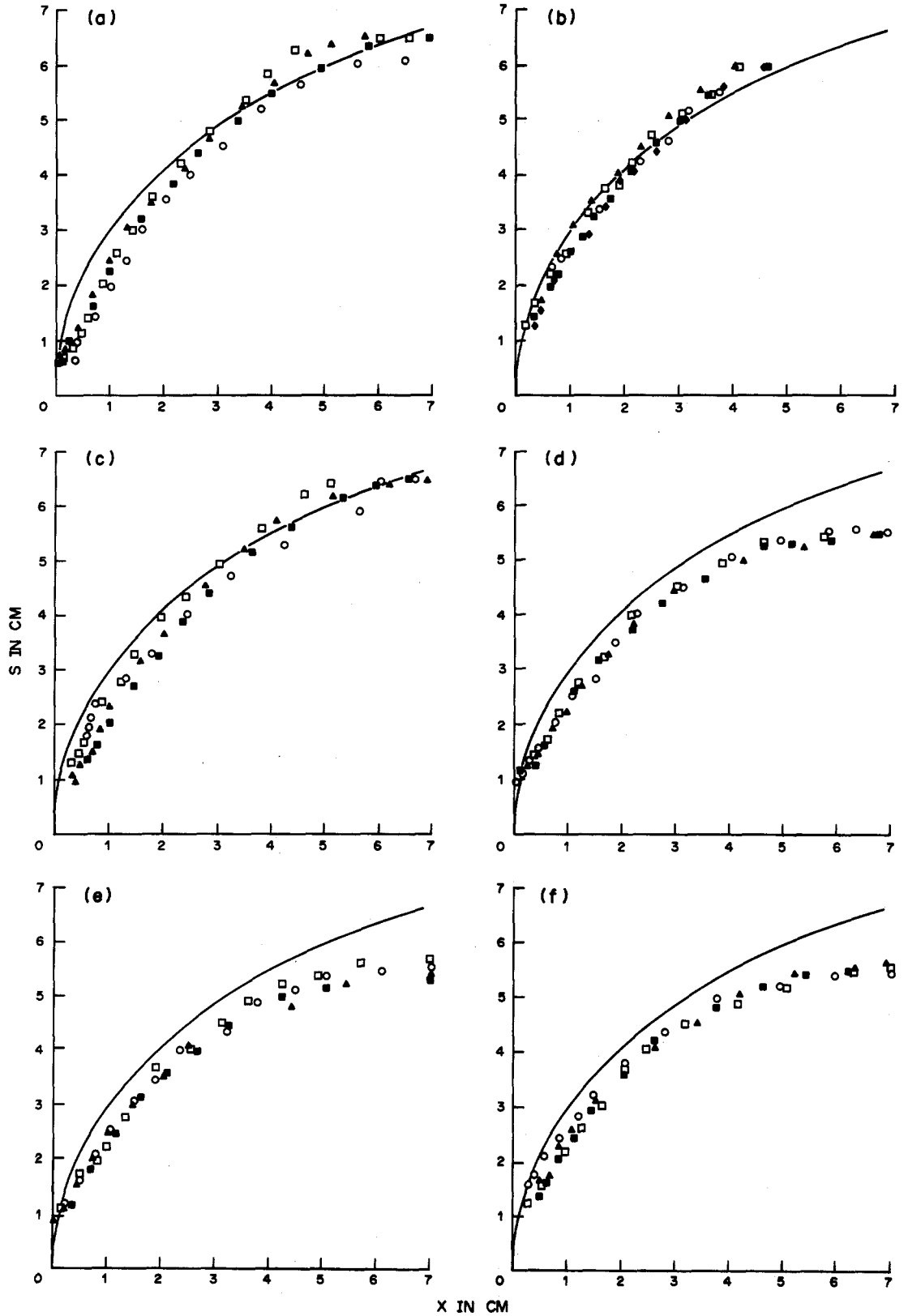

Figure 9. Shape of the nose of a Taylor bubble in an annulus for a stagnant liquid. *Concentric annulus*: (a) $l = 0.113$ m, $U_C = 0.364$ m/s; (b) $l = 0.301$ m, $U_C = 0.377$ m/s; (c) $l = 0.477$ m, $U_C = 0.383$ m/s. *Eccentric annulus*: (d) $l = 0.116$ m, $U_E = 0.340$ m/s; (e) $l = 0.311$ m, $U_E = 0.354$ m/s; (f) $l = 0.521$ m, $U_E = 0.362$ m/s.

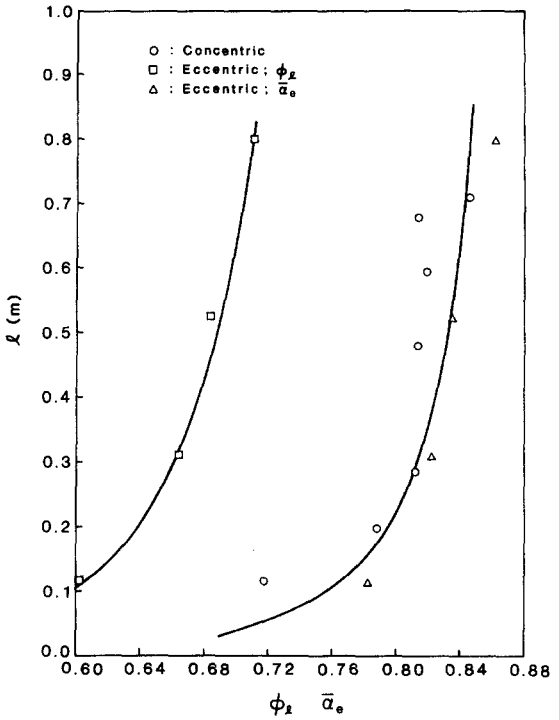

Figure 10. Average ϕ_l values for the concentric and eccentric annulus for a stagnant liquid.

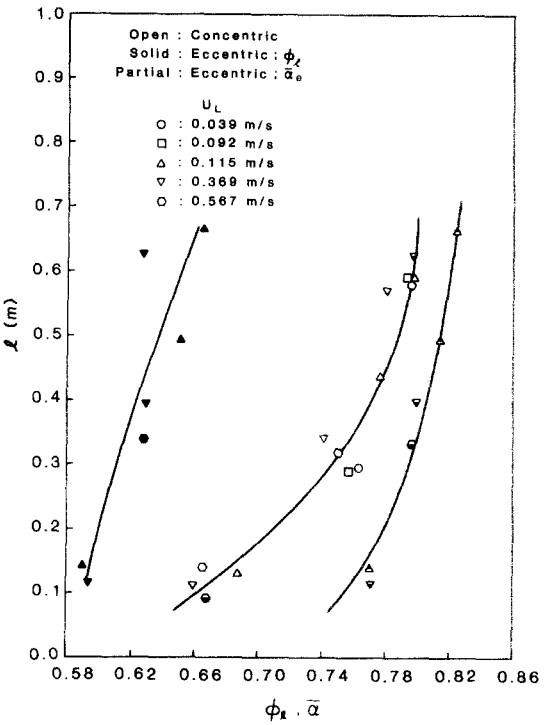

Figure 11. Average ϕ_l values for the concentric and the eccentric annulus for a flowing liquid.

4 m long were injected in the column and never enclosed the inner tube. With the flowing liquid, the fractional area occupied by the bubble in the eccentric configuration was substantially lower than for the concentric annulus. In general, the Taylor bubble appears to occupy less area under flow conditions than under stagnant ones.

Different length Taylor bubbles were injected into stagnant and flowing liquid under the conditions of laminar and turbulent flow (Re ranged from 990 to 3150) and the approximate radial location of the bubble tip in a concentric annulus was determined as discussed above. The results show that typically the bubble tip locates near probe 3 and is towards probe 1 rather than probe 5 (figure 4). The position of the maximum liquid velocity, R_m, for single-phase turbulent flow in an annulus may be determined by the equation proposed by Kays & Leung (1963),

$$\frac{R_m - R_1}{R_2 - R_m} = \left(\frac{R_1}{R_2}\right)^{0.343}, \qquad [12]$$

which yields a position very close to that for laminar flow,

$$R_m = \sqrt{\frac{R_2^2 - R_1^2}{2\ln\left(\frac{R_2}{R_1}\right)}}. \qquad [13]$$

For the annulus of this study, [12] gives $R_m = 31.3$ mm, while [13] gives $R_m = 31.5$ mm which are 1.55–1.57 mm away from the location of probe 3 and towards the centerline. Based on the experimental data and noting that the bubble tip is the point of maximum liquid velocity, it may be concluded that the presence of the bubble causes a shift in the position of the maximum liquid velocity for single-phase flow towards the inner tube, thus creating an even more asymmetric liquid velocity profile. It may be argued, therefore, that the nature of the liquid flow changes in the presence of the Taylor bubble and this fact may explain the large value of the coefficient, in [7], determined for the rise velocity of the Taylor bubble under flow conditions.

RISE VELOCITY OF A TAYLOR BUBBLE IN A CONCENTRIC ANNULUS. THEORETICAL CONSIDERATIONS

Approximate solutions for the rise velocity of the Taylor bubble in a pipe of circular cross section have been developed by a number of authors, as discussed above, using methods based on potential theory. We approach the problem for the concentric annulus in a similar way. First, two types of concentric bubbles are analyzed and it is shown that the theoretically predicted velocities are lower than those observed experimentally. The analysis of the asymmetric bubble is then pursued, with the predicted rise velocity shown to be higher than that for the axisymmetric one and in general accord with measured values. It is suggested that this accounts for the preferred existence of the asymmetric bubble.

A. The axisymmetric bubble

Assume that the Taylor bubble has the shape shown in figure 12. The coordinate system is moving with the bubble so that the bubble is stationary, while far upstream of the bubble tip ($z \to -\infty$) there is uniform downward liquid velocity. The flow is assumed inviscid and irrotational. The Stokes stream function, Ψ, satisfies the equation

$$\frac{\partial^2 \Psi}{\partial z^2} + \frac{\partial^2 \Psi}{\partial r^2} - \frac{1}{r}\frac{\partial \Psi}{\partial r} = 0. \qquad [14]$$

The boundary conditions satisfied by the stream function are

$$\Psi = -\tfrac{1}{2}U^2 \qquad \text{for } z \to \infty, \qquad [15]$$

$$\Psi = -\tfrac{1}{2}UR_1^2 \qquad \text{at } r = R_1 \qquad [16a]$$

and

$$\Psi = -\tfrac{1}{2}UR_2^2 \qquad \text{at } r = R_2, \qquad [16b]$$

since the walls of the annulus are streamlines along which the stream function is constant. In the above equations, U is the bubble rise velocity, R_1 and R_2 are the radii of the inside and outside tube of the annulus and z and r are the axial and radial coordinates. If $\xi = z/R_2$, $\eta = r/R_2$ and $R_i = R_1/R_2$, the solution to [14] subject to boundary conditions [15] and [16] is

$$\Psi(\xi, \eta) = -\tfrac{1}{2}UR_2^2\eta^2 + \sum_{i=1}^{\infty} A_i \exp(\lambda_i \xi) R_2 \eta \left[J_1(\lambda_i \eta) - \frac{J_1(\lambda_i)}{Y_1(\lambda_i)} Y_1(\lambda_i \eta) \right], \qquad [17]$$

where A_i are coefficients to be determined, J_1 and Y_1 are Bessel functions of the first and second kind of order 1, respectively, and λ_i are the eigenvalues, defined as the solution to the equation

$$\frac{J_1(\lambda_i)}{Y_1(\lambda_i)} = \frac{J_1(\lambda_i R_i)}{Y_1(\lambda_i R_i)} = C_i. \qquad [18]$$

The velocity potential, Φ, is given by

$$\Phi = UR_2\xi - \sum_{i=1}^{\infty} A_i \exp(\lambda_i \xi) \left[J_0(\lambda_i \eta) - \frac{J_1(\lambda_i)}{Y_1(\lambda_i)} Y_0(\lambda_i \eta) \right], \qquad [19]$$

where J_0 and Y_0 are Bessel functions of zero order. The flow has a uniform velocity for $\xi \to -\infty (\Phi = UR_2\xi)$, while the radial liquid velocity, v, becomes zero at $\eta = R_i$ and $\eta = 1$, as required by the statement of the problem. At $\xi = 0$, the bubble forms a "rim" of radius $\eta = R_i$ (see figure 12). Following Davies & Taylor (1950), only the first term in the series solution is retained, thus giving

$$\Phi = UR_2\xi - A_1 \exp(\lambda_1 \xi)[J_0(\lambda_1 \eta) - C_1 Y_0(\lambda_1 \eta)] \qquad [20]$$

and

$$\Psi = -\tfrac{1}{2}UR_2^2\eta^2 + A_1 R_2 \eta \exp(\lambda_1 \xi)[J_1(\lambda_1 \eta) - C_1 Y_1(\lambda_1 \eta)], \qquad [21]$$

where

$$C_1 = \frac{J_1(\lambda_1)}{Y_1(\lambda_1)} = \frac{J_1(\lambda_1 R_i)}{Y_1(\lambda_1 R_i)} \quad [22]$$

and λ_1 is the solution to [22]. The bubble surface is defined as

$$\Psi(\xi, \eta) = \Psi(0, R_i) = -\tfrac{1}{2} U R_2^2 R_i^2$$

and, therefore,

$$-\tfrac{1}{2} U R_2^2 \eta^2 + A_1 R_2 \eta \exp(\lambda_1 \xi)[J_1(\lambda_1 \eta) - C_1 Y_1(\lambda_1 \eta)] = -\tfrac{1}{2} U R_2^2 R_i^2. \quad [23]$$

The axial velocity component, u, is

$$u = U - \frac{A_1 \lambda_1}{R_2} \exp(\lambda_1 \xi)[J_0(\lambda_1 \eta) - C_1 Y_0(\lambda_1 \eta)], \quad [24]$$

while the radial velocity component, v is

$$v = \frac{A_1 \lambda_1}{R_2} \exp(\lambda_1 \xi)[J_1(\lambda_1 \eta) - C_1 Y_1(\lambda_1 \eta)]. \quad [25]$$

For $\eta = R_i$, [25] and [22] give $v(0, R_i) = 0$, while [24] gives

$$u(0, R_i) = U - \frac{A_1 \lambda_1}{R_2}[J_0(\lambda_1 R_i) - C_1 Y_0(\lambda_1 R_i)]. \quad [26]$$

Since there is no liquid flow across the bubble interface, the rim of the bubble is a stagnation region and therefore

$$u(0, R_i) = 0 \Rightarrow \frac{A_1 \lambda_1}{R_2} = \frac{U}{J_0(\lambda_1 R_i) - C_1 Y_0(\lambda_1 R_i)}. \quad [27]$$

The pressure inside the bubble is constant. Bernoulli's equation between the rim of the bubble and any point (η, ξ) on the bubble surface gives

$$\left(\frac{\partial \Phi}{\partial \xi}\right)^2 + \left(\frac{\partial \Phi}{\partial \eta}\right)^2 = 2 g R_2^3 \xi, \quad [28]$$

where g is the acceleration of gravity. Evaluation of the partial derivatives and substitution yields

$$\frac{U}{\sqrt{2gR_2}} = \sqrt{\xi}\left\{\left[1 - \exp(\lambda_1 \xi)\frac{J_0(\lambda_1 \eta) - C_1 Y_0(\lambda_1 \eta)}{J_0(\lambda_1 R_i) - C_1 Y_0(\lambda_1 R_i)}\right]^2 + \left[\exp(\lambda_1 \xi)\frac{J_1(\lambda_1 \eta) - C_1 Y_1(\lambda_1 \eta)}{J_0(\lambda_1 R_i) - C_1 Y_0(\lambda_1 R_i)}\right]^2\right\}^{-1/2}. \quad [29]$$

Equations [22], [23] and [29] provide the general solution for the rise velocity of large gas bubbles rising through stagnant liquids in a vertical concentric annulus to the first approximation. The problem for the circular tube (Davies & Taylor 1950) is a special case and can be derived from the above solution by setting $R_1 = 0$ ($R_i = 0$).

Because the series solution was truncated at the first term, full closure of the problem is not possible. There are two equations, [23] and [29], and three unknowns, namely η, ξ and U. Following Davies & Taylor (1950), the pressure condition (expressed by [29]) may be satisfied at one radial position η^* and hence at one axial position ξ^*. The solution procedure was therefore to choose a value for η^*, determine the value of ξ^* from [23] and calculate the Froude number, Fr, based on the diameter of the outside tube, D_2,

$$\mathrm{Fr} = \frac{U}{\sqrt{gD_2}}, \quad [30]$$

from [29].

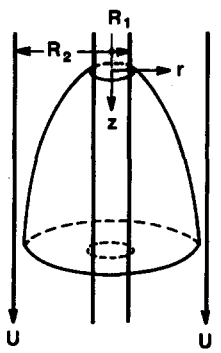

Figure 12. Axisymmetric Taylor bubble rising in a concentric annulus. First model.

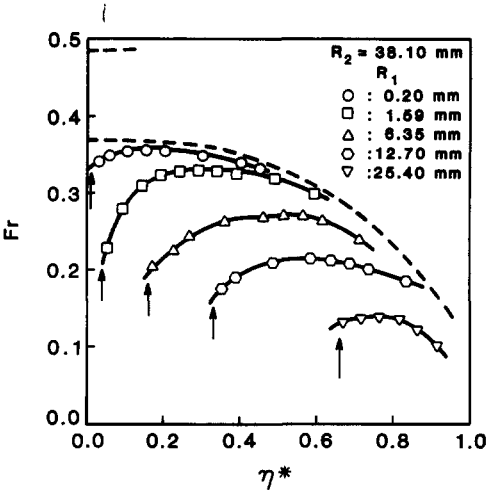

Figure 13. Fr vs η^* for an axisymmetric Taylor bubble rising in a tube and a concentric annulus.

Davies & Taylor (1950) chose the value of $\eta^* = 0.5$ and derived an Fr (based on the tube diameter D) equal to 0.328. If, however, a series of values is assumed, then the results, shown in figure 13, indicate that Fr attains a limiting value of Fr = 0.361 as $\eta^* \to 0$, in better agreement with the value obtained by Dumitrescu (1943) ([1], with $K = 0.35$).

The results for an axisymmetric bubble rising in annuli with $R_2 = 3.81$ cm and different R_1 (R_1 ranged from 0.02 to 2.54 cm), are also present in figure 13. The arrows indicate the minimum value of $\eta^* = R_1/R_2$. It should be noted that the test section used in the experiments reported above corresponds to $R_1 = 2.54$ cm and $R_2 = 3.8$ cm. The results indicate that as η^* increases, Fr goes through a maximum which no longer occurs at the minimum value of η^*, the case for a circular tube. The rise velocity of an axisymmetric bubble in a concentric annulus decreases as the inside tube diameter increases and is smaller than the corresponding empty tube case. These results are counter to the experimental data presented above as well as data by Griffith (1964), Rader *et al.* (1975) and Sadatomi *et al.* (1982).

Another possible axisymmetric bubble shape is shown in figure 14. The top of the bubble is defined by the coordinates $(0, R_m)$. There are two radial positions, R_{11} and R_{12} for every axial position ($z > 0$), which define the bubble surface. An analysis similar to the one presented above was carried out. The minimum number of terms that can be retained from the series solution is two, while the pressure condition is satisfied at one axial and hence two radial positions. The final solution, a system of six equations with seven unknowns, with $\eta_m = R_m/R_2$ chosen as the free parameter, is similar to that previously obtained and is not presented here. Solutions were found to exist within a narrow range of η_m values. The results for $R_2 = 3.81$ cm and four inside tube radii are shown in figure 15. Inspection of figure 15 indicates that this type of axisymmetric bubble (figure 14) yields the same trend as the type shown in figure 12, i.e. the bubble rise velocity decreases as the diameter of the inside tube increases, in contradiction to the experimental data.

The above analysis is based on the assumptions that the bubble is axisymmetric and that the flow around the rim of the bubble is inviscid. Since the assumption of inviscid flow leads to acceptable results for flow in circular tubes and between parallel plates, it seems likely that the cause for the error in predictions is due to the assumption of symmetry. Experiments in annuli with inside tube radii varying from 0.16 to 2.32 cm and an outside tube radius of 3.81 cm showed that full closure of the bubble to obtain a symmetric shape never occurred. If one adopts the argument of Garabedian (1957), that the stable bubble will rise the fastest, it may be argued that since a symmetric bubble rises at a smaller velocity than that measured experimentally, a symmetric bubble in an annulus is unstable and therefore never observed in real systems. In what follows, a model which approximates the true situation will be presented.

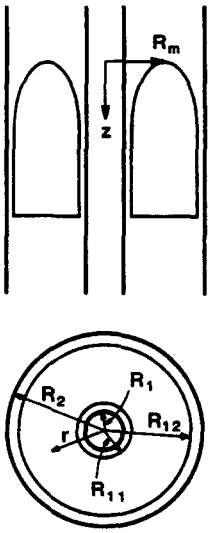

Figure 14. Axisymmetric Taylor bubble rising in a concentric annulus. Second model.

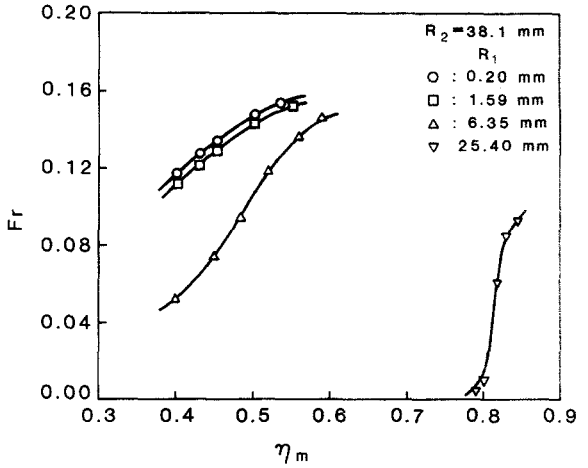

Figure 15. Fr vs η_m for an axisymmetric Taylor bubble rising in a concentric annulus.

B. The asymmetric bubble

The experimental results described above indicated that the forward portion of bubbles rising in concentric annuli is elliptic, irrespective of the bubble length. If the annulus is unbent in the direction indicated by the arrows in figure 7 and the resulting bubble is projected on a vertical plane passing through the bubble tip, one derives the situation shown in figure 16. The width of the channel, $2h$, represents the perimeter of the annulus based on the radial distance of the bubble tip from the center of the tube, R_b,

$$2h = 2\pi R_b. \qquad [31]$$

It is assumed that the bubble shape is elliptic and the flow is inviscid. The coordinate system is moving upwards with a velocity U, the unknown bubble rise velocity. Following Grace & Harrison (1967), the complex potential for flow around an elliptic cylinder is given by

$$W = U(a+b)[\cosh(\xi - \xi_0)\cos\eta + i\sinh(\xi - \xi_0)\sin\eta], \qquad [32]$$

where a and b are the major and the minor axis of the ellipse and ξ and η are the elliptic coordinates defined as:

$$c^2 = a^2 - b^2, \qquad \text{focal distance}, \qquad [33]$$

$$x' = a - x = c\cosh\xi\cos\eta, \qquad [34]$$

$$y = c\sinh\xi\sin\eta \qquad [35]$$

and

$$\frac{x'^2}{c^2\cosh^2\xi} + \frac{y^2}{c^2\sinh^2\xi} = 1. \qquad [36]$$

For $\xi = \xi_0$, a constant, the point (x, y) lies on an ellipse whose semiaxes are given by

$$a = c\cosh\xi_0, \qquad [37]$$

$$b = c\sinh\xi_0. \qquad [38]$$

If $z = x' + iy$; $\zeta = \xi + i\eta$, the liquid velocity, q, is given by

$$q = \frac{dW}{dz} = \frac{U(a+b)}{c}\frac{\sinh(\xi - \xi_0)}{\sinh\zeta}. \qquad [39]$$

Expanding the hyperbolics and equating real and imaginary parts, the vertical and lateral velocity components may be shown to be

$$u = \frac{U(a+b)}{c} \frac{\sinh(\xi - \xi_0)\sinh \xi + \cosh \xi_0 \sin^2 \eta}{\sinh^2 \xi + \sin^2 \eta} \quad [40]$$

and

$$v = \frac{U(a+b)\sinh \xi_0 \sin \eta \cos \eta}{\sinh^2 \xi + \sin^2 \eta}. \quad [41]$$

The bubble tip is defined as $x = 0$, $y = 0$ or $\xi = \xi_0$, $\eta = 0$, so that at the tip $u = 0$ and $v = 0$ and the tip is a stagnation point. The magnitude of the velocity at the bubble surface, $\xi = \xi_0$, is given by

$$q_0^2 = (u^2 + v^2)_0 = \frac{U^2(a+b)}{(a-b)} \frac{\sin^2 \eta}{\sinh^2 \xi_0 + \sin^2 \eta}. \quad [42]$$

The pressure inside the bubble is constant and application of Bernoulli's equation between the stagnation point and any point on the bubble surface gives

$$q_0^2 - 2ga(1 - \cos \eta) = 0. \quad [43]$$

Combination of [42] and [43] yields

$$U^2 = \frac{a-b}{a+b} 2ga \frac{1 - \cos \eta}{\sin^2 \eta} (\sinh^2 \xi_0 + \sin^2 \eta). \quad [44]$$

Equation [44] is satisfied close to the stagnation point (i.e. $\eta \to 0$) and the final result can be shown to be

$$U = \frac{b}{a+b} \sqrt{ga}. \quad [45]$$

Equation [45] is similar to the equation derived by Grace & Harrison (1967) and relates the rise velocity of elliptical bubbles rising in isolation to the bubble dimensions. In general, however, the bubble dimensions are not known. The following analysis relates the bubble dimensions to the channel dimensions so that the rise velocity may then be determined without knowledge of the actual bubble dimensions.

At the plane $x = a$, the value of η is $\eta = \pi/2$ for every y and hence, the lateral velocity component v, is zero everywhere, [41]. Noting also that the bubble is symmetric in the y-direction, the vertical velocity component, u, is the same for every y and therefore, has the same value as at the bubble surface. An alternative way of arriving at the same result is to note that the liquid flow is between two planes of zero shear stress and hence, there is no velocity variation in the y-direction and therefore the vertical liquid velocity is the same as the velocity at the bubble surface.

Based on the above discussion, the liquid velocity at the plane $x = a$, U_x, is given by

$$U_x = q_0 = \sqrt{2gx} \qquad \text{at } x = a. \quad [46]$$

Dumitrescu (1943) assumed that the radial component of the liquid velocity far downstream from the bubble tip is negligible and, hence, the average liquid velocity is given by [46] for the axisymmetric bubble rising in a tube. This assumption is, however, questionable at the point where the solution was obtained (Brown 1965). For the model presented here, however, no assumption is made and [46] is a result of the particular flow situation.

A mass balance between any point far upstream from the bubble and $x = a$ gives

$$U = \frac{h-b}{h} \sqrt{2ga}. \quad [47]$$

Inspection of figures 7 and 16 shows that

$$\frac{b}{h} = \frac{\theta}{\pi} = \phi. \quad [48]$$

Combination [45], [47] and [48] yields

$$\frac{a}{b} = \frac{1}{(1-\phi)\sqrt{2}} - 1 \qquad [49]$$

and

$$\mathrm{Fr}_h = \frac{U}{\sqrt{2gh}} = \sqrt{-\phi^3 + \left(2 - \frac{\sqrt{2}}{2}\right)\phi^2 + \left(\frac{\sqrt{2}}{2} - 1\right)\phi}. \qquad [50]$$

In order for the argument of the square root to be positive, ϕ must take values within the range $0.2929 < \phi < 1$. Since a and b were assumed to be the major and the minor axis of the ellipse, $a/b > 1$, hence, the range of ϕ values is $0.6464 < \phi < 1$. It can be shown that Fr_h has a maximum at this condition:

$$\phi_m = 0.7278, \qquad \mathrm{Fr}_m = 0.2935, \qquad [51]$$

where the subscript m denotes the maximum condition. It should be noted that ϕ_m is not the maximum value of ϕ observed along the back of the Taylor bubble. Rather it represents the value of $\phi = b/h$ which exists at the origin of the ellipse for that particular ellipse which results in the maximum rise velocity. We accept Garabedian's (1957) speculation that the bubbles observed experimentally are those which yield the maximum velocity. Thus, the applicable Fr is $\mathrm{Fr}_m = 0.2935$.

In order to compute a rise velocity to compare with, experiments are necessary to select h. If L_t denotes the radial distance from the inside tube to the location of the bubble tip, then

$$h = \pi(R_1 + L_t). \qquad [52]$$

The simplest choice, in the absence of data, is

$$L_t = \frac{(R_2 - R_1)}{2}, \qquad [53]$$

a bubble whose tip is located halfway between the inside and outside tube walls. For the annulus of this study, [53] yields $h = 9.97$ cm. In fact, experimental results, presented above, suggest that $0.218 \leqslant L_t \leqslant 0.436$ cm, which yields $8.66 \leqslant h \leqslant 9.35$ cm. For the experiments described above, use of $\mathrm{Fr}_m = 0.2935$ gives a predicted rise velocity of $0.382 \leqslant U \leqslant 0.397$ m/s compared to the experimentally measured average value of 0.37 m/s. Thus, the error ranges from 3.2 to 7.3% high.

Equations [51] and [52] were used to predict the rise velocity of Taylor bubbles in annuli studied by previous investigators. The comparison is shown in figure 17. In the absence of other data, h was calculated using [53]. The prediction of the theory is considered satisfactory for all the cases which cover a wide range of annuli tube diameters (R_1 ranged from 0.75 to 10.08 cm and R_2 ranged from 1.50 to 12.17 cm).

It is now necessary to test the assumption that the forward portion of bubbles rising in concentric annuli is part of an ellipse. The ellipse defined by $\phi_m = 0.7278$ and $h = 9.97$ cm is given by

$$a = 11.60 \text{ cm}, \qquad b = 7.26 \text{ cm} \qquad [54a]$$

and

$$\frac{(a-x)^2}{a^2} + \frac{y^2}{b^2} = 1. \qquad [54b]$$

Equation [54] is shown as the solid line in figures 9(a–f). The plots indicate reasonable agreement between the theory and experiments for the concentric annulus and for distances up to ~7 cm from the bubble tip. The data for the eccentric annulus agrees with [54] over a smaller axial distance but the agreement may still be considered satisfactory. The fact that the rise velocity did not change appreciably with eccentricity, as the data indicated, may also be deduced from the above figures where the same ellipse approximates equally well the nose of the bubble rising in a concentric or an eccentric annulus. It should also be noted that if the value of h was chosen as the value indicated

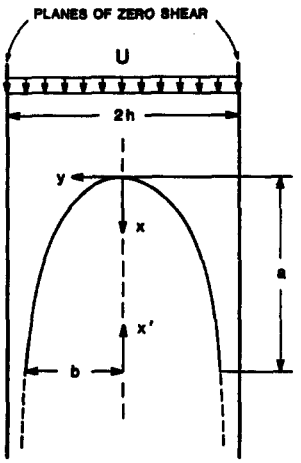

Figure 16. Elliptic Taylor bubble rising between parallel planes.

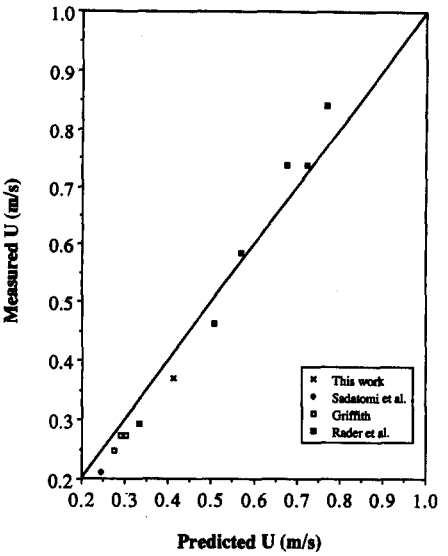

Figure 17. Comparison of predicted with measured rise velocity in a concentric annulus.

by experiment, an even better agreement of the theory with the experimental data would be derived both for the concentric and the eccentric annulus.

Grace & Harrison (1967) observed that small capped bubbles rising between parallel planes take up an elliptic shape when they enclosed a rod as they rose, while they were spherical in the absence of the rods. Based on measurements of the bubble dimensions, they found good agreement between theory and experiment. In general, however, the bubble dimensions are not known. They showed that elliptical bubbles rise faster than spherical bubbles. Therefore, elliptical bubbles should be observed in practice, if one adopts the argument of Garabedian (1957). This, however, does not occur for bubbles rising in circular tubes or between parallel plates because theory shows that elongated bodies placed in a moving stream are subject to destabilizing moments (Milne-Thomson 1968). Hence, bubbles rising in these geometries as well as in isolation, take up the spherical shape. Grace & Harrison (1967) speculated that the presence of the rod provides a stabilizing couple and therefore the bubbles take up the elliptic shape.

The theory presented above shows that an elliptic asymmetric bubble rises faster than an axisymmetric one in a concentric annulus. Furthermore, no destabilizing moments are likely to exist since the bubble occupies more than 70% of the periphery and the center tube seems to stabilize the bubble, as in the case studied by Grace & Harrison (1967). Thus, elliptical Taylor bubbles are observed rather than spherical. In an extension of these ideas the bubble dimensions were related to the equipment size and the bubble velocity can then be determined from the inside and outside tube radii of the concentric annulus.

CONCLUSION

Bubbles rising through liquids in vertical annuli are radially asymmetric, rise faster than the corresponding circular tube and never occupy the whole cross-sectional area. Experimental data indicates that the forward portion of bubbles rising through stagnant liquid takes an approximate elliptic shape, in contrast to bubbles rising in other geometries (tube, parallel planes) where the forward portion is nearly spherical.

A theory has been developed which predicts the velocity of an elliptic bubble rising through stagnant liquid in a concentric annulus. The predictions agree well with experiment from this study as well as results reported by previous investigators.

The propagation velocity of bubbles rising in flowing liquid or during slug flow is the sum of the rise velocity through stagnant liquid and a contribution due to bulk motion of the fluid ahead of the bubble tip. The latter is higher than in the circular tube and it is plausible that in the presence

of the bubble, the maximum liquid velocity ahead of the bubble tip increases from its single-phase flow value.

Acknowledgement—This work was supported by Schlumberger-Doll Research.

REFERENCES

BENDIKSEN, K. H. 1984 An experimental investigation of the motion of long bubbles in inclined tubes. *Int. J. Multiphase Flow* **10,** 467–483.

BENDIKSEN, K. H. 1985 On the motion of long bubbles in vertical tubes. *Int. J. Multiphase Flow* **11,** 797–812.

BIRKHOFF, G. & CARTER, D. 1957 Rising plane bubbles. *J. Math. Mech.* **6,** 769–779.

BROWN, R. A. S. 1965 The mechanics of large gas bubbles in tubes. *Can. J. chem. Engng* **43,** 217–223.

COLLINS, R. A. S. 1965 A simple model of the plane gas bubble in a finite liquid. *J. Fluid Mech.* **22,** 736–771.

COLLINS, R., DE MOARES, F. F., DAVIDSON, J. F. & HARRISON, D. 1978 The motion of a large gas bubble rising through liquid flowing in a tube. *J. Fluid Mech.* **89,** 497–514.

COUET, B., STRUMULO, G. S. & DUKLER, A. E. 1986 Modeling two dimensional large bubbles in rectangular channels of finite width. *Phys. Fluids* **29,** 2367–2373.

DAVIES, R. M. & TAYLOR, G. 1950 The mechanics of large bubbles rising through extended liquids and through liquids in tubes. *Proc. R. Soc.* **A200,** 375–390.

DUKLER, A. E. & TAITEL, Y. 1986 Flow pattern transitions in gas–liquid systems. Measurements and modeling. In *Advances in Multiphase Flow*, Vol. 2 (Edited by ZUBER, N., HEWITT, G. F. & DELHAYE, J. M.). McGraw-Hill, New York.

DUMITRESCU, D. T. 1943 Strömung an einer luftblase im senkreshter rohr. *Z. angew. Math. Mech.* **23,** 139–149. (English translation by OLSCHER, W. G.)

FERNANDES, R. C., SEMIAT, R. & DUKLER, A. E. 1983 Hydrodynamic model for gas–liquid slug flow in tubes. *AIChE Jl* **28,** 981–989.

GARABEDIAN, P. 1957 On steady-state bubbles generated by Taylor instability. *Proc. R. Soc.* **A241,** 423–431.

GRACE, J. R. & HARRISON, D. 1967 The influence of bubble shape on the rise velocities of large bubbles. *Chem. Engng Sci.* **22,** 1337–1347.

GRIFFITH, P. 1964 The prediction of low-quality voids. *J. Heat Transfer* **86,** 327–333.

KAYS, W. M. & LEUNG, E. Y. 1963 Heat transfer in annular passages—hydrodynamically developed turbulent flow with arbitrarily prescribed heat flux. *Int. J. Heat Mass Transfer* **6,** 537–557.

KELESSIDIS, V. C. & DUKLER, A. E. 1989 Modeling flow pattern transitions for upward gas–liquid flow in vertical concentric and eccentric annuli. *Int. J. Multiphase Flow* **15,** 173–191.

MAO, Z.-S. & DUKLER, A. E. 1990 Motion of Taylor bubbles in vertical tubes. I. Numerical simulation for the shape and rise velocity in stagnant and flowing liquid. *J. comput. Phys.* Accepted for publication.

MILNE-THOMSON, L. M. 1968 *Theoretical Hydrodynamics*, 5th edn. Arrowsmith, London.

NICKENS, H. V. & YANNITELL, D. W. 1987 The effects of surface tension and viscosity on the rise velocity of a large gas bubble in a closed, vertical liquid-filled tube. *Int. J. Multiphase Flow* **13,** 57–69.

NICKLIN, D. J., WILKES, M. A. & DAVIDSON, J. F. 1962 Two phase flow in vertical tubes. *Trans. Instn chem. Engrs* **40,** 61–68.

RADER, D. W., BOURGOYONE, A. T. JR & WARD, R. H. 1975 Factors affecting bubble rise velocity of gas kicks. *J. Petrol. Technol.* **27,** 571–584.

SADATOMI, M., SATO, Y. & SARUWATARI, S. 1982 Two phase flow in vertical non-circular channels. *Int. J. Multiphase Flow* **6,** 641–655.

VANDEN-BROEK, J.-M. 1984 Bubbles rising in a tube and falling from a nozzle. *Phys. Fluids* **27,** 1090–1093.